Journal of Urban and Environmental Engineering, v.6, n.2, p.123-131

ISSN 1982-3932
doi: 10.4090/juee.2012.v6n2.123131

Journal of Urban and Environmental Engineering

www.journal-uee.org

CUCKOO SEARCH VIA LÉVY FLIGHTS FOR OPTIMIZATION OF A PHYSICALLY-BASED RUNOFF-EROSION MODEL

Celso A. G. Santos[1*], Paula K. M. M. Freire[2] and Sudhanshu K. Mishra[3]

[1]Department of Civil and Environmental Engineering, Federal University of Paraíba.
[2]Master student of Urban and Environmental Engineering, Federal University of Paraíba.
[3]North-Eastern Hill University, Shillong, India.

Received 2 September 2012; received in revised form 10 December 2012; accepted 20 December 2012

Abstract: This paper aims to calibrate a physically-based, event-oriented runoff-erosion model by means of a global optimization method known as cuckoo-host co-evolution (CHC) which has co-evolutionary changes incorporated into the traditional cuckoo search algorithm. The physically-based erosion model that was chosen to be optimized here is the watershed erosion simulation program (WESP), which was developed for small semiarid basins to simulate runoff and erosion processes. The optimization technique was tested with the field data collected in an experimental watershed located in a semiarid region of Brazil, and such technique showed to be effective in order to locate the optimal erosion parameter values. On the basis of these results, such values for a semiarid region are given, which could be recommended as an initial estimate for other similar areas.

Keywords: Cuckoo search; runoff-erosion simulation; optimization.

* Correspondence to: Celso A. G. Santos, Tel.: +55 83 3216 7684 Ext 27. E-mail: celso@ct.ufpb.br

INTRODUCTION

Physically-based erosion models seem to be a useful tool for basin simulation. However, they have parameters which cannot be directly measured in the field. In this context, many algorithms for function optimization are employed to find values for those parameters. However, it is difficult to assure that the final value for the parameter is not a result of either a local minimum or another trap. Therefore, more robust algorithms are required to estimate the parameter's final value (Soares Júnior *et al.*, 2010; Santos *et al.*, 2011).

There are different methods for solving an optimization problem. Some of these methods are inspired from natural processes. The Cuckoo search is a new evolutionary optimization algorithm which was inspired by the obligate brood parasitism of some cuckoo species by laying their eggs in the nests of other host birds. Some host birds can engage direct conflict with the intruding cuckoos, e.g., if a host bird discovers the eggs are not their own, it will either throw these alien eggs away or simply abandon its nest and build a new nest elsewhere. Environmental features and the immigration of societies (groups) of cuckoos hopefully lead them to converge and find the best environment for breeding and reproduction. This best environment is the global maximum of objective functions.

This paper utilizes the cuckoo search for optimize the parameters of the WESP runoff-erosion model to estimate runoff and sediment yield in an experimental basin in a semiarid area of northeastern Brazil.

It is divided in seven sections. In the first one, it was given a brief introduction of the work. In second section, a review about the cuckoo search optimization. The third section contains tests with some mathematic function. In the fourth section, the WESP is explained. The fifth section contains information about the studied area. In the sixth section, the application and optimization results are shown. In the seventh and last section, some conclusions are presented.

CUCKOO SEARCH OPTIMIZATION

A novel method of global optimization based on the behavior of cuckoos was proposed by Yang & Deb (2009). Cuckoos are brood parasites that lay their eggs in the nests of other birds (such as crows) who serve as hosts to hatch their eggs. It was shown that the so-called "cuckoo search" algorithm is quite effective for global optimization. The works of Yang & Deb (2010), Civicioglu & Besdok (2011), Rajabioun (2011) and Valian *et al.* (2011) further confirmed that the "cuckoo search" algorithm, in its original or improved version, proves to be very effective. The method has been successfully tested on a large number of benchmark functions of varied dimensions and difficulty levels.

The original "cuckoo search algorithm" of Yang & Deb (2009) or any of its variants is based on the idea how cuckoos lay their eggs in the host nests; how, if not detected and destroyed, the eggs are hatched to chicks by the hosts; how the cuckoo chicks hatched by the host later join the population of cuckoos and how a search algorithm based on such a scheme can be used to find the global optimum of a function. To implement this search scheme, Yang & Deb (2009) formulated the following idealized rules: (a) Each cuckoo lays a single egg into a randomly chosen host nest from among *n* nests; (b) The nests with better quality eggs (implying better fitness value of the function concerned), if not detected, would be hatched to grow into the cuckoo chicks, who would join the next generation; (c) The number of available host nests is fixed. The host can detect the alien egg with a probability [0, 1] and, if detected, it will either abandon the nest and build a new nest elsewhere or destroy the egg; (d) When generating new solutions $\left(x_i^{(t+1)}\right)$ from the old one $\left(x_i^{(t)}\right)$, Lévy flight is performed with the parameter $1 < \beta < 3$ and, thus,

$$x_i^{(t+1)} = x_i^{(t)} + \alpha \otimes \mathrm{Levy}(\beta) \tag{1}$$

for, say cuckoo i; $\alpha = O(1)$, $\otimes$ means the Hadamard product operator. The Lévy flight is a type of random walk which has a power law step length distribution with a heavy tail. It has been found (Brown *et al.*, 2007; Pavlyukevich, 2007) that Lévy flights is an oft-observed random walk in many real life situations (Viswanathan *et al.*, 1996; 1999; 2002).

Researchers in ornithology have found that brood parasitism leads to co-evolution of the parasites as well as the hosts (Rothstein, 1990; Krüger *et al.*, 2009). Mishra (2012) incorporated the co-evolutionary changes into the "Cuckoo Search" algorithm and tested the efficiency of the two populations (of the cuckoos and the hosts) in finding the global optimum of some benchmark functions. This new suggested algorithm was named as the "Cuckoo-Host Co-Evolution" or CHC algorithm.

To elucidate, let there be n parasites and equally many (although not necessarily) hosts. Each parasite individual would be represented by a point (x in m-dimensional space) and similarly each host individual would be represented by a point (y in m-dimensions). These points may be randomly generated and would lie in the domain of the function to be optimized.

Each cuckoo would take a Lévy flight and if its post-flight fitness is better than its pre-flight fitness, it would randomly choose a host nest that has not as yet been invaded by another cuckoo and the quality of the host eggs are inferior to the cuckoo egg. If this condition is not met, it would not lay any egg in the host nest. The egg of a successful parasite may, however, be detected (with probability p) by the host and be destroyed. If not detected, however, it would be hatched in the host nest and eventually join the cuckoo population. Only the best n cuckoos, however, would enter into the next generation. The Lévy flight will follow the attractive rule as given hereunder:

$$x_{ij}^{(t+1)} = x_{ij}^{t} + \left[\alpha(r_1 - 0.5) \times \text{Levy}(\beta)\right] \times \left[\left(y_{ij}^{t} - x_{ij}^{t}\right)\right] \quad (2)$$

where $\alpha = 0.0001 + (r_x)^2; \beta = 3/2$. Each un-invaded host (crow) would take a Lévy flight and if its post-flight fitness is better than its pre-flight fitness, it would update itself, else it would retain its old status. The Lévy flight will follow the repulsive rule as given hereunder:

$$y_{ij}^{(t+1)} = y_{ij}^{t} + \left[\omega(r_2 - 0.5) \times \text{Levy}(\gamma)\right] \times \left[\left(x_{ij}^{t} - y_{ij}^{t}\right)\right] \quad (3)$$

where $\varpi = 0.0001 + (r_y)^2; \gamma = 5/3$. It may be noted that due to the smaller value of β, the cuckoos will have wider flight ranges than the host (crows) will have (Gutowski, 2001; Mishra, 2012).

On completion of this process the cuckoo and the host populations would enter the next generation (iteration). At each next iteration (t), the probability of rejection (of the cuckoo eggs in the host nest) will increase under the rule as:

$$p^{(t)} = a + b\left(\frac{t}{\max t}\right) \quad (4)$$

such that the probability will be almost $(a+b)$ at last. In this, a could be a small number such as 0.01 and b could be 0.6 or even 0.7. In this simple case, the probability of rejection increases linearly. However, the probability of rejection may also follow the Gompertz growth curve given by

$$P^{(t)} = b\left\{\exp\left[-2\exp\left(\frac{-0.00001}{1+\ln\left(1+\left|\text{best}F_x - \text{best}F_y\right|\right)}\right)t\right]\right\} \quad (5)$$

where b may be as high as 0.7. This algorithm is co-evolutionary on two accounts: first that both – the invaders (cuckoos) and the hosts (crows, say) – take levy flights in view of their cohort and themselves (y_{ij}^{t} and x_{ij}^{t}) and, secondly, that at every subsequent iteration, the probability of rejection increases. Also, since only the un-invaded hosts take Lévy flights, their strategies depend on the success of the invaders.

TESTS WITH MATHEMATICAL FUNCTIONS

This section describes some test functions used in the evaluating performance of the CHC algorithm. These functions were extracted from the literature (Mishra, 2006) about genetic algorithms, evolutionary strategies and global optimization. **Table 1** shows the results of the CHC algorithm to optimize these functions.

Shubert function

The 2-dimension Shubert function (**Fig. 1a**) has 760 local minima, 18 of which are global minima with –186.73067. They are unevenly spaced.

$$f(x_1, x_2) = \sum_{j=1}^{5} j\cos[(j+1)x_1 + j] \sum_{j=1}^{5} j\cos[(j+1)x_2 + j] \quad (6)$$

where $x_i \leq 10$, $i = 1, 2$.

Penholder function

This is a multi-modal function (**Fig. 1b**) with the minima equal to –0.96354, given as

$$f(x_1, x_2) = -\exp\left[-\left|\cos(x_1)\cos(x_2)e^{\left|1-\frac{(x_1^2+x_2^2)^{0.5}}{\pi}\right|}\right|^{-1}\right] \quad (7)$$

where the search domain is $-11 \leq x_i \leq 11$, $i = 1, 2$.

Bird function

This is a bi-modal function (**Fig. 1c**) with minimum equal to −106.764537, given as

$$f(x_1, x_2) = \sin(x_1)e^{(1-\cos(x_2))^2} + \cos(x_2)e^{(1-\sin(x_1))^2} + (x_1 + x_2)^2 \quad (8)$$

where the search domain is $-2\pi \leq x_i \leq 2\pi$, $i = 1, 2$.

Himmelblau function

This is a multi-modal function (**Fig. 1d**), used to test the performance of optimization algorithms. The function is defined by:

$$f(x_1, x_2) = \left(x_1^2 + x_2 - 11\right)^2 + \left(x_1 + x_2^2 - 7\right)^2 \quad (9)$$

where $-10 \leq x_i \leq 10$, $i = 1, 2$.

Table 1. Global minima for the testing functions using the CHC algorithm

Function	x_1	x_2	$f_{min}(x_1, x_2)$
Shubert	–0.8003	–1.4251	–186.7309
Penholder	9.6462	–9.6462	–0.9635
Bird	–1.5821	–3.1302	–106.7645
Himmelblau	3.0000	2.0000	0.0000
Multimodal	0.0000	0.0000	–1.0000
Rosenbrock	1.0000	1.0000	0.0000

This function has four identical local minima equal to 0. The locations of all the minima can be found analytically. However, because they are roots of cubic polynomials, when written in terms of radicals, the expressions are somewhat complicated.

Multimodal function

This function (**Fig. 1e**), with minimum equal to –1, is defined by:

$$f(x_1, x_2) = \cos(x_1)\cos(x_2)\exp\left[-\left(x_1^2 + x_2^2\right)^{\frac{2}{4}}\right] \quad (10)$$

where the search domain is $-10 \leq x_i \leq 10$, $i = 1, 2$.

Rosenbrock function

This function (**Fig. 1f**) is a non-convex function used as a performance test problem for optimization algorithms. It is also known as Rosenbrock's valley or Rosenbrock's banana function.

The global minimum is inside a long, narrow, parabolic shaped flat valley. To find the valley is trivial. To converge to the global minimum, however, is difficult.

It is defined by:

$$f(x_1, x_2) = (1 - x_1)^2 + 100\left(x_2 + x_1^2\right)^2 \quad (11)$$

It has a global minimum at $x_1 = 1$ and $x_2 = 1$ where $f(x_1, x_2) = 0$. A different coefficient of the second term is sometimes given, but this does not affect the position of the global minimum.

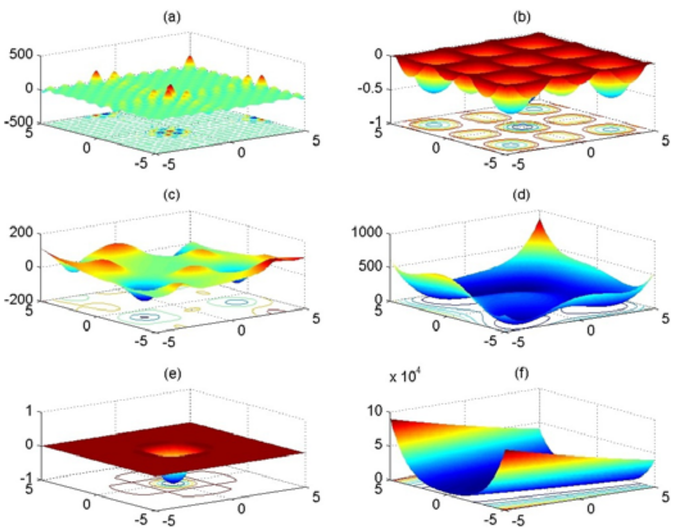

Fig. 1 The 3D view (f, x_1, x_2) for (a) Shubert function, (b) Penholder function, (c) Bird function, (d) Himmelblau function, (e) Multimodal function and (f) Rosenbrock function.

WESP MODEL

The WESP model (Lopes & Lane, 1988) is a physically-based distributed model, which computes runoff and sediment yield based on kinematic waves approximation for the surface flow due to excess rainfall r_e (m/s) in small basins. The rainfall excess is computed by the subtraction of the infiltration rate $f(t)$ from the rainfall intensity I, i.e., $r_e = I - f(t)$. The infiltration process is modeled with the Green-Ampt equation (Green & Ampt, 1911):

$$f(t) = K_s\left(1 + \frac{N_s}{F(t)}\right) \quad (12)$$

in which, K_s is the effective saturated soil hydraulic conductivity (m/s), $F(t)$ is the cumulative depth of infiltrated water (m), N_s is the soil moisture-tension parameter. The surface flow is considered to be either the overland flow on planes or channel flow.

Overland flow

The spatially varied overland flow is considered one-dimensional and is described by Manning's turbulent flow equation as:

$$u = \frac{1}{n} R_H^{2/3} S_f^{1/2} \quad (13)$$

in which u is the local mean flow velocity (m/s), $R_H(x,t)$ is the hydraulic radius (m), S_f is the friction slope and n is the Manning friction factor. Thus, the local velocity for plane flow is obtained considering the hydraulic radius equal to the depth of flow ($R_H = h$) and using the kinematic wave approximation resulting in the friction slope being equal to the plane slope ($S_0 = S_f$):

$$u = \alpha' h^{m-1} \quad (14)$$

where h is the depth of flow (m), α' is a parameter related to surface slope and roughness, equal to $(1/n)S_0^{1/2}$, and m is a geometry parameter whose value is set to 5/3 for wide rectangles. The equation of continuity for the one-dimensional plane can be written as:

$$\frac{\partial h}{\partial t} + \alpha' m h^{m-1}\frac{\partial h}{\partial x} = r_e \quad (15)$$

From **Eqs (14)** and **(15)**, the overland flow velocity and depth (u, h) is calculated for a given rainfall excess r_e.

Sediment transport is considered as the erosion rate in the plane reduced by the deposition rate within the reach. The erosion occurs due to raindrop impact as well as surface shear. Thus, the continuity equation for sediment transport is expressed as:

$$\frac{\partial(ch)}{\partial t}+\frac{\partial(cuh)}{\partial x}=e_I+e_R-d \qquad (16)$$

where c is the sediment concentration in the surface flow (kg/m^3), e_I is the rate of sediment erosion due to rainfall impact (kg s/m^2), e_R is the erosion rate due to shear stress (kg s/m^2), and d is the rate of sediment deposition (kg s/m^2). The rate of sediment erosion due to rainfall impact e_I is a function of the rate of detachment by raindrop impact and the rate of transport of sediment particles by shallow flow. A simple functional form of detachment by raindrop impact could use rainfall intensity as a measure of the erosivity of raindrop impact (Foster, 1982), and in order to include the process of sediment transport by shallow flow on hillslopes, Lane & Shirley (1985) included rainfall and expressed e_I as:

$$e_I = K_I\, I\, r_e \qquad (17)$$

where K_I is the soil detachability parameter (kg s/m^4). The rate of sediment erosion due to shear stress e_R is expressed by an entrainment rate proportional to a power of the average shear stress acting on the soil surface (Croley, 1982; Foster, 1982) as:

$$e_R = K_R\, \tau^{1.5} \qquad (18)$$

where K_R is a soil erodibility factor for shear (kg m/N$^{1.5}$ s), and τ is the effective shear stress (N/m^2), which is given by $\tau = \gamma h S_f$, γ being the specific weight of water (N/m^3). Finally, the rate of sediment deposition d in **Eq. (16)** is not only the deposition of the particular sediment per unit of area and per unit of time, but it also represents the rate at which the column of suspension loses solids per unit of time, and is expressed as (Einstein, 1968):

$$d = \varepsilon_p V_s c \qquad (19)$$

where ε_p is a coefficient that depends on the sediment and fluid properties, set to 0.5 in this study based on Davis (1978), $c(x,t)$ is the plane sediment concentration in transport (kg/m^3), and V_s is the particle fall velocity (m/s) computed by Rubey's equation:

$$V_s = F_o\sqrt{\frac{(\gamma_s-\gamma)}{\gamma}g d_s} \qquad (20)$$

and,

$$F_o=\sqrt{\frac{2}{3}+\frac{36\nu^2}{g d_s^3\left(\frac{\gamma_s}{\gamma}-1\right)}}-\sqrt{\frac{36\nu^2}{g d_s^3\left(\frac{\gamma_s}{\gamma}-1\right)}} \qquad (21)$$

where γ_s is the specific weight of sediment (N/m^3), ν is the kinematic viscosity of water (m^2/s), d_s is the mean diameter of the sediment (m), and g is the acceleration of gravity (m/s^2).

Channel flow

The concentrated flow in the channels is also described by continuity and momentum equations. The momentum equation could be reduced to the discharge equation with the kinematic wave approximation as:

$$Q = \alpha' A R_H^{\,m-1} \qquad (22)$$

where Q is the discharge (m^3/s), and A is the cross-sectional area of flow (m²). The continuity equation for the channel flow is given by:

$$\frac{\partial A}{\partial t}+\frac{\partial Q}{\partial x}=q_A \qquad (23)$$

where q_A is the lateral inflow per unit length of channel. **Equations (22)** and **(23)** enable the calculation of channel flow. Since the effect of rainfall impact is negligible in the channel, the continuity equation for the sediment is expressed without the rainfall impact component by:

$$\frac{\partial AC}{\partial t}+\frac{\partial CQ}{\partial x}=q_s+e_r-d_c \qquad (24)$$

where $C(x,t)$ is the sediment concentration in transport in the channel (kg/m²), q_s is the lateral sediment inflow into the channel (kg s/m), d_c is the rate of sediment deposition in the channel (kg s/m), and e_r is the erosion rate of the channel bed material (kg s/m). The components of the net sediment flux for the channel segment are given as follows: the erosion rate of the channel bed material e_r is obtained from a general equation, initially developed for bed-load transport capacity (Croley, 1982; Foster, 1982):

$$e_r = a(\tau-\tau_c)^{1.5} \qquad (25)$$

where a is the sediment erodibility parameter (kg m²/s), and τ_c is the critical shear stress for sediment entrainment (N/m^2), which is given by $\tau_c = \delta(\gamma_s-\gamma)d_s$, where δ is a coefficient, set to 0.047 in the present study, γ_s is the specific weight of sediment (N/m^3), and d_s is the mean diameter of sediments (m). The rate of sediment deposition within the channel d_c (kg s/m) in **Eq. (24)** is expressed by (Mehta, 1983):

$$d_c = \varepsilon_c T_W V_s C \qquad (26)$$

where ε_c is the deposition parameter for channels, considered as unity in the present case based on the study of Einstein (1968), and T_W is the top width of the channel flow (m). From **Eq. (24)**, sediment transport rate (CQ) could be calculated for the overland flow with A and Q obtained from **Eq. (23)**.

THE STUDIED AREA

The WESP model was utilized to simulate runoff and erosion in a bare micro-basin, which is one of the four micro-basins of the Sumé Experimental Watershed, in the northeastern Brazil. Its mean slope, area and perimeter are 7.1%, 0.48 ha, and 302 m, respectively. This experimental watershed was operated from 1982 to 1991 by SUDENE (Superintendency of Northeast Development, Brazil), ORSTOM (French Office of Scientific Research and Technology for Overseas Development) and UFPB (Federal University of Paraíba, Brazil) to obtain field data for calculating the runoff and sediment yield produced by rainfall in a natural environment (Cadier *et al.*, 1983).

The experimental basin includes four micro-basins, nine erosion plots of 100 m², and several micro-plots of 1 m² operated under simulated rainfall within a sub-basin of 10.7 km². The surface conditions and the slope were varied among the plots and micro-basins. Four standard rain gauges and two recording rain gauges, installed close to the micro-basins and plots, provided the rainfall data. At the outlet of the micro-basins, a rectangular collector was installed for the measurement of water and sediment discharge. A 90º triangular weir at the end of the collector allowed the measurement of outflow discharges. The collector held all the surface runoff and sediment discharges for most of the low to medium rainfall events, thereby providing a means for accurate runoff and sediment measurement. Based on the work of Santos *et al.* (2003, 2011, 2012), 21 events were selected between 1987 and 1988 and 17 more events were selected between 1989 and 1991 making up a total of 38 events. These periods were chosen because the micro-basin was maintained bare during them, under controlled conditions of maintenance.

APPLICATION AND RESULTS

Optimization of the runoff-erosion model

A scheme of planes and channels was firstly selected to represent the studied area. The schematization of the micro-basin in 10 elements has been reported (Santos *et al.*, 1994) to be the best scheme to represent the area, thus this schematization was selected in this studied.

In the WESP model some parameter values are fixed a priori such as the specific weight of water (9.8 kN/m³), the specific weight of sediment (2.6×10^4 N/m³) and Manning friction factor, which was assumed as 0.02 for planes and 0.03 for channels based on the soil type, its grain size composition and surface characteristics. However, there are some parameters that are specific for this area which should be determined by field tests such as the mean diameter of sediments d_s whose value was assumed to be equal to d_{50} (0.5 mm) and the saturated soil hydraulic conductivity K_s whose average value was set equal to 5.0 mm/h.

The values of the other four remaining parameter (N_s, a, K_R and K_I) should be based either on the literature or determined by calibration with an optimization process. The first parameter to be calibrated in the WESP model is the soil moisture-tension parameter N_s, in **Eq. (12)**, which was calibrated by minimized the following runoff objective function:

$$J_L = \left| \frac{L_o - L_c}{L_o} \right| \tag{27}$$

where L_o is the observed runoff depth (mm) and L_c is the calculated one (mm).

The other three parameters (a, K_R and K_I) are related to the erosion process, so the optimization had to be done according to the adjustment of computed and observed sediment yield data. Since there are no universally applicable values for these three erosion parameters, they were optimized using the CHC method. The range in which these parameters could vary was chosen to be 0.001 to 200 mm for N_s, 0.0001 to 0.9 kg m² for a, 1.0 to 3.0 kg m/N$^{1.5}$ s for K_R, and 0.1×10^8 to 10.0×10^8 kg s/m^4 for K_I, whose initial values of the runoff and erosion parameters were randomly set.

The erosion objective function J_E to be minimized was:

$$J_E = \left| \frac{E_o - E_c}{E_o} \right| \tag{28}$$

where E_o is the observed sediment yield (kg) and E_c is the calculated one (kg). The optimization for the 38 events agreed 100% with each event (**Table 2**).

The mean values of the erosion parameters are computed as $a = 0.0441$ kg m²/s, $K_R = 1.4594$ kg m/N$^{1.5}$, and $K_I = 4.4533 \times 10^8$ kg s/m^4. However, since the larger event data ($E_o > 100$ kg) are more accurate than the smallest ones, the mean parameter values for such events are computed as well, as show in **Table 3**, i.e., $a = 0.0147$ kg m²/s, $K_R = 1.3666$ kg m/N$^{1.5}$ and $K_I = 4.3619 \times 10^8$ kg s/m^4, which are more appropriate to be used as the mean parameters for the studied region. Both means (mean using all events and mean using the events larger than 100 kg) were used to run new simulation. As one can observed from **Fig. 2**, the computed sediment yield using the mean parameters of the events with $E_o < 100$ kg tends to overestimate.

Figure 3 shows the simulation results for the sediment yield using the mean values of events larger than 100 kg. This figure shows some acceptable degree of agreement, except for few events, which can be attributed to some errors in the observed data, especially for the smallest sediment yield events (**Fig. 4**), in which high relative errors can be observed.

Table 2. Optimized values of the erosion parameters a, K_R and K_I, in which the events with E_o > 100 kg are highlighted

Date (dd/mm/yy)	N_s (m)	a (kg m^2/s)	K_R (kg m/N$^{1.5}$s)	$K_I \times 10^8$ (kg s/m^4)	L_o (mm)	L_c (mm)	E_o (kg)	E_c (kg)
07/02/87	0.0731	0.0028	1.3779	1.8658	0.190	0.1900	4.092	4.092
12/02/87	0.0170	0.1201	1.6759	2.2573	0.060	0.0630	19.188	19.188
02/03/87	0.0291	0.0060	1.1628	6.5578	0.060	0.0560	0.967	0.967
02/05/87	0.0317	0.0267	1.8672	2.0008	2.310	2.3100	1214.522	1214.522
01/06/87	0.0605	0.2040	1.8414	2.7746	0.003	0.0030	0.941	0.941
29/06/87	0.0018	0.0058	1.1208	2.8859	1.370	1.3709	168.184	168.184
04/07/87	0.0059	0.8912	1.4312	0.1000	0.010	0.0070	5.273	5.273
20/01/88	0.0883	0.0132	1.1497	0.5720	5.710	5.7121	2061.862	2061.862
23/02/88	0.0079	0.0209	1.0934	7.4482	1.580	1.5800	568.490	568.490
12/03/88	0.0050	0.0065	2.6470	1.3698	0.120	0.1210	4.378	4.378
14/03/88	0.0051	0.0122	1.0914	6.7962	5.670	5.6690	1875.531	1875.531
19/03/88	0.0060	0.0159	1.0464	6.1307	1.690	1.6890	580.076	580.079
24/03/88	0.0058	0.0034	1.0575	0.5845	13.520	13.5208	4019.038	4019.038
05/04/88	0.0161	0.0092	1.1397	5.7054	10.600	10.6000	3615.399	3615.399
08/04/88	0.0132	0.0025	1.2346	4.1006	7.230	7.2310	1286.652	1286.652
19/04/88	0.0131	0.0136	1.0212	4.1592	9.630	9.6300	3504.550	3504.550
30/04/88	0.0319	0.0050	1.4362	7.5800	5.360	5.3609	887.390	887.390
06/05/88	0.0058	0.0008	2.3822	3.1465	7.820	7.8190	898.472	898.472
13/07/88	0.0040	0.0077	1.0785	4.4710	0.450	0.4460	40.732	40.732
16/07/88	0.0021	0.0440	1.1282	4.6012	0.220	0.2190	83.564	83.564
25/07/88	0.0065	0.0089	2.8179	7.2435	0.030	0.0300	0.494	0.494
14/01/89	0.0121	0.0048	1.7430	5.4746	0.010	0.0100	0.042	0.042
01/03/89	0.0127	0.0032	1.4585	2.9535	6.750	6.7500	918.502	918.502
27/03/89	0.0143	0.0991	1.5093	1.8920	0.440	0.4400	527.504	527.504
05/04/89	0.0014	0.0007	1.1388	3.4633	0.310	0.3100	2.460	2.460
21/04/89	0.0004	0.0076	1.3151	6.2437	3.750	3.7500	674.211	674.211
04/05/89	0.0047	0.0332	1.5624	4.0370	0.370	0.3697	128.991	128.991
09/05/89	0.0075	0.0106	1.0601	2.8706	4.790	4.7900	1186.172	1186.172
11/05/89	0.0019	0.0164	2.1559	4.3085	0.580	0.5801	167.674	167.674
03/07/89	0.0048	0.0014	1.2053	5.5358	0.070	0.0700	0.395	0.395
08/02/90	0.0414	0.0024	1.3464	6.9744	0.130	0.1300	1.768	1.768
10/02/90	0.0004	0.0023	1.1543	6.2507	5.090	5.0900	404.357	404.357
28/04/90	0.0023	0.0015	1.2081	7.5355	0.090	0.0900	0.572	0.572
28/05/90	0.0067	0.0046	1.9485	7.1202	5.170	5.1700	793.946	793.946
06/07/90	0.0036	0.0107	2.1006	7.2209	0.010	0.0060	0.057	0.057
19/10/90	0.0034	0.0029	1.1438	1.1570	10.160	10.1570	1443.650	1443.650
18/05/91	0.0196	0.0085	1.4907	5.8172	0.560	0.5600	54.402	54.402
19/05/91	0.0045	0.0021	1.1163	8.0175	4.060	4.0597	245.539	245.539

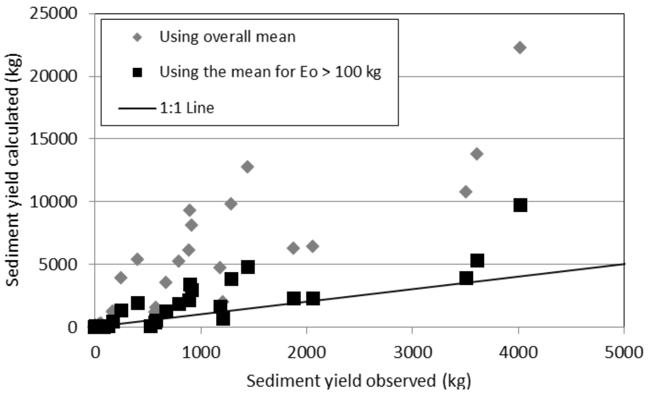

Fig. 2 Scatter plot of errors as ratios of observed and calculated sediment yield.

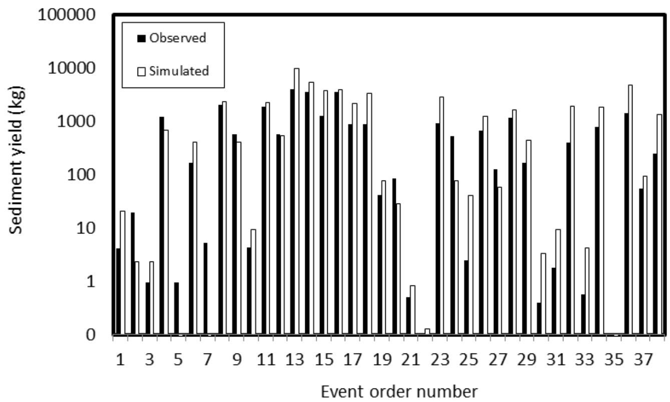

Fig. 3 Observed and simulated sediment yield using the mean erosion parameters.

Table 3. Main statistics for the erosion parameters a, K_R and K_I

Statistics	All Events			Events with E_o > 100 kg		
	a (kg m^2/s)	K_R (kg m/N$^{1.5}$ s)	$K_I \times 10^8$ (kg s/m^4)	a (kg m^2/s)	K_R (kg m/N$^{1.5}$ s)	$K_I \times 10^8$ (kg s/m^4)
Arithmetic mean	0.0441	1.4594	4.4533	0.0147	1.3666	4.3619
Median	0.0077	1.2749	4.3898	0.0092	1.1520	4.1299
Harmonic mean	0.0041	1.3529	1.6491	0.0047	1.2852	2.4433
Geometric mean	0.0089	1.4006	3.4756	0.0082	1.3219	3.5112
Range	0.8905	1.7967	7.9175	0.0983	1.3610	7.4455
First quartile	0.0032	1.1309	2.7986	0.0034	1.0991	2.8744
Third quartile	0.0159	1.6475	6.4810	0.0159	1.4966	6.2490
Interquartile range	0.0127	0.5167	3.6824	0.0125	0.3975	3.3745
Median abs. deviation	0.0615	0.3563	2.0059	0.0118	0.3080	2.0033
Variance	0.0221	0.2145	5.4396	0.0004	0.1530	5.5943
Standard deviation	0.1485	0.4632	2.3323	0.0211	0.3912	2.3652
Coef. of variation	3.3681	0.3174	0.5237	1.4378	0.2863	0.5422
Skewness	5.4747	1.4529	–0.1968	3.4814	1.4214	–0.0487
Kurtosis	31.5038	1.5203	–1.1971	13.7588	1.1291	–1.2379
Excess kurtosis	28.5038	–1.4797	–4.1971	10.7588	–1.8709	–4.2379

CONCLUSIONS

A physically-based erosion model was used to simulate the runoff and sediment yield form a micro-basin in a semiarid region of Brazil. The conclusions are as follows: (1) the physically-based erosion model was shown to be useful for simulation in small areas; (2) the CHC algorithm was proved to be a robust optimization technique; (3) the soil moisture-tension parameter N_s depends also on the initial moisture content then it should be different for each rainfall event, (4) the channel erosion parameter a, the soil detachability factor K_R, and sediment entrainment parameter by rainfall impact K_I are obtained as constant for almost all rainfall events in the experimental basin. Although the mean parameter values using all events could be used is further studies, the mean values obtained using the larger event data (E_o > 100 kg) seems to be more appropriate since the observed data are more accurate than the smallest ones. Thus, the values a = 0.0147 kg m²/s, K_R = 1.3666 kg m/N$^{1.5}$ and K_I = 4.3619 × 10^8 kg s/m^4 should be used as the mean parameters for the studied region.

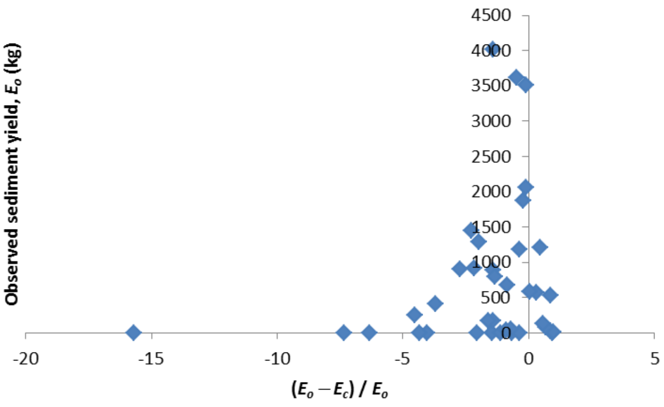

Fig. 4 Scatter plot of errors as ratios of observed sediment yield and mean relative error.

Acknowledgment The writers wish to thank Dr V. Lopes of Texas State University (US) for providing the WESP model and to the UFCG (Federal University of Campina Grande, Brazil), SUDENE (Brazil) and IRD (*Institut de Recherche pour le Développement*, France) for the field data. The financial support provided by CNPq (National Council for Scientific and Technological Development, Brazil) is gratefully acknowledged.

REFERENCES

Brown, C., Liebovitch, L.S. & Glendon, R. (2007) Lévy flights in Dobe Ju/'hoansi foraging patterns. *Human Ecol.* **35**(129–138).

Civicioglu, P. & Besdok, E. (2011) A conceptual comparison of the Cuckoo-search, particle swarm optimization, differential evolution and artificial bee colony algorithms, *Artif. Intell. Rev.*, doi: 10.1007/s10462-011-9276-0.

Croley, T.E. (1982) Unsteady overland sedimentation. *J. Hydrol.*, **56**(1982), 325–346.

Davis, S.S. (1978) Deposition of nonuniform sediment by overland flow on concave slopes. MSc Thesis, Purdue University, West Lafayette, IN, p. 137.

Einstein, H.A. (1968) Deposition of suspended particles in a gravel bed. *J. Hydraul. Div. ASCE*, **94**(HY5), 1197–1205.

Foster, G.R. (1982) Modeling the erosion process. In: C.T. Haan, H.P. Johnson, & D.L. Brakensiek (editors), Hydrologic modeling of small watersheds, *Am. Soc. Agr. Eng.*, 295–380.

Green, W.H. & Ampt, G.A. (1911) Studies on soil physics, I. The flow of air and water through soils. *J. Agr. Sci.*, **4**(1), 1–24.

Gutowski, M. (2001) Lévy flights as an underlying mechanism for global optimization algorithms, arXiv:math-ph/0106003v1[4 Jun 2001]. http://arxiv.org/abs/math-ph/0106003v1.

Krüger, O., Sorenson, M.D. & Davies, N.B. (2009) Does coevolution promote species richness in parasitic cuckoos? *Proc. R. Soc. B*, **276**, 3871–3879.

Lane, L.J. & Shirley, E.D. (1985) Erosion and sediment yield equations: solutions for overland flow. Paper presented at the *Workshop on USLE Replacement*, Nat. Soil Erosion Lab., West Lafayette, IN, p. 22.

Lopes, V.L., & Lane, L.J. (1988) Modeling sedimentation processes in small watersheds. In: Sediment Budgets. *IAHS Publ.* **174**, 497–508.

Mehta, A.J. (1983) Characterization tests for cohesive sediments. In: H. T. Shen (editor), *Proc. Conf. on Frontiers in Hydraul. Engng.* (ed. By H.T. Shen), 79–84. ASCE/MIT, Cambridge, Mass., USA.

Mishra, S.K. (2006) Some new test functions for global optimization and performance of repulsive particle swarm method. Available at SSRN: http://ssrn.com/abstract=926132.

Fuches Viswanathan, G.M., Afanasyev, V., Buldyrev, S.V., Murphy, E.J., Prince, P.A., & Stanley, H.E. (1996) Lévy flight search patterns of wandering Albatrosses, *Nature*, **381**, 413–415.

Mishra, S.K. (2012) Global optimization of some difficult benchmark functions by cuckoo-host co-evolution meta-heuristics. Available at SSRN: http://ssrn.com/abstract=2128079.

Pavlyukevich, I. (2007) Lévy flights, non-local search and simulated annealing, *J. Computational Physics*, **226**, 1830–1844.

Rajabioun, R. (2011) Cuckoo optimization algorithm, *Applied Soft. Computing*, **11**, 5508–5518.

Rothstein, S.I. (1990) A model system for coevolution: avian brood parasitism, *Ann. Rev. Ecol. Syst.* **21**, 481–508.

Santos, C.A.G., Freire, P.K.M.M., & Arruda, P.M. (2012) Application of a simulated annealing optimization to a physically-based erosion model. *Water Sci. and Technology*, **66**(10), 2099–2108. doi: 10.2166/wst.2012.426.

Santos, C.A.G., Freire, P.K.M.M., Mishra, S.K. & Soares Júnior, A. (2011) Application of a particle swarm optimization to the tank model. *IAHS Publ.* **347**, 114–120.

Santos, C.A.G., Freire, P.K.M.M., Silva, R.M., Arruda, P.M. & Mishra, S.K. (2011) Influence of the catchment discretization on the optimization of runoff-erosion modeling. *J. Urban Environ. Engng*, **5**(2), 91–102. doi: 10.4090/juee.2011.v5n2.091102.

Santos, C.A.G., Srinivasan, V.S., Suzuki, K. & Watanabe, M. (2003) Application of an optimization technique to a physically based erosion model. Hydrol. Process. 17(5), 989–1003. doi: 10.1002/hyp.1176

Santos, C.A.G., Suzuki, K., Watanabe, M. & Srinivasan, V.S. (1994) Optimization of coefficients in runoff-erosion modeling by Standardized Powell method, *J. Hydrosci. and Hydraul. Engng*, **12**(1), 67–78.

Viswanathan, G.M., Bartumeus, F., Buldyrev, S.V., Catalan, J., Fulco, U.L., Havlin, S., da Luz, M.G.E., Lyra, M.L., Raposo, E.P., & Stanley, H.E. (2002) Lévy flight random searches in biological phenomena, *Physica - A*, **314**, 208–213.

Viswanathan, G.M., Buldyrev, S.V., Havlin, S., da Luz, M.G.E., Raposo, E.P., & Stanley, H.E. (1999) Optimizing the success of random searches, *Nature*, **401**, 911–914.

Yang, X.S. & Deb, S. (2009) Cuckoo search via Lévy flights, Proc. World Congress on Nature & Biologically Inspired Computing (NaBIC 2009, India), *IEEE Publications*, 210–214.

Yang, X.S. & Deb, S. (2010) Engineering optimisation by cuckoo search, *Int. J. Math. Modell. and Numerical Optimisation*, **1**(4): 330–343. doi: 10.1504/IJMMNO.2010.035430.